EURASIP Journal on Applied Signal Processing 2005:2, 193–206

A Low-Complexity Source Encoding Assisted Multiple Access Protocol for Voice/Data Integrated Networks

Andres Kwasinski
Department of Electrical and Computer Engineering and The Institute for Systems Research, University of Maryland, College Park, MD 20742, USA
Email: ak@umd.edu

Mehdi Alasti
Department of Electrical and Computer Engineering and The Institute for Systems Research, University of Maryland, College Park, MD 20742, USA
Email: mehdi@umd.edu

K. J. Ray Liu
Department of Electrical and Computer Engineering and The Institute for Systems Research, University of Maryland, College Park, MD 20742, USA
Email: kjrliu@umd.edu

Nariman Farvardin
Department of Electrical and Computer Engineering and The Institute for Systems Research, University of Maryland, College Park, MD 20742, USA
Email: farvar@umd.edu

Received 22 August 2003; Revised 19 May 2004

We present and evaluate the performance of a reduced complexity variation to the source encoding assisted multiple access (SEAMA) protocol for integrating voice and data over a wireless network. This protocol, denoted as slow movable-boundary SEAMA (SMB-SEAMA), uses the same embedded and multistate voice encoder used in the original SEAMA protocol. However, in SMB-SEAMA, the movable voice/data boundary is not set based on the frame-by-frame bandwidth demand of the voice subsystem, but on the number of ongoing voice calls and the acceptable average distortion level. This results in a protocol that, at the network layer, is packet switched for both voice and data; however, from the data traffic point of view, the voice looks like circuit switched. Analytical results show that SMB-SEAMA is a very efficient MAC protocol and presents a model for analyzing the performance of queuing systems with a variable number of servers, each with a constant service time. Consequently, while reducing the refreshing rate of the movable boundary by three orders of magnitude, simulation results demonstrate that SMB-SEAMA does not significantly degrade the system performance (less than 8% reduction in throughput) and it still performs better than packet reservation multiple access (PRMA), the other known packet-switched scheme, which updates the boundary during every transmit frame.

Keywords and phrases: TDMA, embedded voice coding, packet-switched wireless network, voice-data boundary setting, voice-data integration.

1. INTRODUCTION

In a resource-limited wireless network, the medium access control (MAC) protocol design plays an essential role in integrating different services (e.g., voice and data) and satisfying each service demands while providing high network utilization. While end-users evaluate network performance in terms of the perceived quality (regardless of how it is defined), network operators and designers face the conflicting need to satisfy end-users' demands and assure high network utilization. At the root of this problem is the need to consider the design problem at two different layers of the communication link: the application layer and the network layer. Because of these inherently conflicting constrains on different layers, a cross-layer design can provide the best solution.

A circuit-switched network (e.g., a TDM network) assigns a dedicated channel to an admitted call for the whole duration of the call. While this approach guarantees quality of service (QoS) for real-time traffic, it also results in large network inefficiencies and underutilizations.

A successful MAC protocol operates across different layers of the communication link to achieve high network efficiency by employing statistical multiplexing. In a voice/data wireless network, the utilization can be increased by exploiting the time-varying characteristic of speech at the application layer in conjunction with statistical multiplexing and movable-boundary schemes [1, 2] at the network layer. The idea is to logically separate voice and data subsystems by a movable boundary, the slots[1] left unused by voice are made available to data. For example, the wireless integrated multiple access (WIMA) protocol [1] takes advantage of the variations in the number of voice calls by incorporating a movable boundary for the voice subsystem that assigns the free slots to data traffic. This MAC protocol is circuit switched for voice subsystem and packet switched for data subsystem.

Packet-switched protocols take advantage of the variations in the output rate of real-time traffic (e.g., voice) to assign the network resources among users more efficiently. Packet reservation multiple access (PRMA) protocol [3, 4], uses the talk spurt/silence model of voice [5], and only calls in a talk spurt can access the channel. Similar to WIMA, PRMA separates voice and data subsystems with a movable boundary. Unlike WIMA, in PRMA both voice and data subsystems are packet switched. In every frame, the movable boundary in PRMA depends on states of all the voice calls. Thus, we consider this as fast movable boundary (FMB) as opposed to slow movable boundary (SMB) in WIMA.

The source encoding assisted multiple access (SEAMA) protocol exploits source encoder characteristics for voice/data integration in a wireless network [6]. SEAMA increases network utilization while it provides the desired QoS for applications. At the application layer, SEAMA employs an embedded multistate (multirate) voice encoder. An embedded voice encoder has the property that a truncated version of its output bit stream can be used to generate a coarser description of the original input signal. SEAMA assigns bandwidth to ongoing calls based on the state of the encoders (state of the calls). SEAMA resolves overflows by selectively dropping packets from the embedded bit stream of some calls, according to an optimal scheduling policy. As a result, SEAMA achieves a significant gain in network utilization, for example, a 100% gain compared to a circuit-switched network and at least a 20% compared to PRMA [6]. Moreover, the quality of the voice traffic degrades gracefully by increasing the number of admitted calls. At the network layer, and similar to PRMA, SEAMA is packet switched for both voice and data and it incorporates an FMB, that is, the movable boundary is updated every frame.

SEAMA (with FMB) provides high network utilization, however, it adds to the complexity when compared to WIMA (with SMB). In SEAMA and PRMA the state information of all voice calls are needed to determine the FMB; in contrast, in WIMA the number of ongoing voice calls is enough to obtain the SMB. The challenge is to develop a low-complexity MAC protocol with SMB that provides a performance comparable with SEAMA.

This paper proposes a low-complexity intelligent MAC protocol that is a modification to SEAMA for supporting voice and data in a wireless communication network. More precisely, the proposed protocol reduces the refreshing rate of voice/data boundary by three orders of magnitude when compared to SEAMA and PRMA, yet, its performance is close to SEAMA and still better than PRMA.

We propose a variation of SEAMA, SMB-SEAMA, that uses an SMB. Our goal is to design, analyze, and evaluate the performance of such new MAC protocol. At the application layer, SMB-SEAMA uses the same voice encoder (embedded and multistate) employed in SEAMA. At the network layer, SMB-SEAMA is packet switched for both voice and data; however, from data traffic point of view, voice looks like circuit switched. In other words, the SMB depends only on the number of voice calls. In essence, SMB-SEAMA still achieves the high network utilization provided by SEAMA while it reduces the complexity by using an SMB. Even more, analytical results also indicate that SMB-SEAMA behaves as a highly efficient MAC protocol. Simulation results show that SMB-SEAMA does not significantly degrade the system performance (less than 8% reduction in throughput) when compared to FMB-SEAMA.

The rest of this paper is organized as follows. Section 2 presents the description of the SMB-SEAMA protocol. Section 3 provides the design of the movable-boundary scheme. In Section 4, we present mathematical analysis of the movable-boundary setting and both the voice and data subsystem performance. In the case of the voice subsection, we study the statistical characteristics of the average distortion for a given number of calls. Our work in the data subsection leads to the mathematical study of the behavior of a multiserver queuing system with fixed service time and infinite waiting queue where the number of servers changes over time following some random process (a truncated Poisson in our case). Section 5 presents the simulation results and comparisons to PRMA and between the slow and the fast movable schemes. Finally, Section 6 draws some conclusions.

2. DESCRIPTION OF SEAMA

Next, we provide a brief description of SEAMA. Further details can be found in [6]. Consider a TDMA integrated voice and data network. Because we are focusing on design issues at the application and network layers we will assume error-free uplink and downlink channels with negligible propagation delay. On the uplink, communication is carried over fixed length frames of T_f seconds, each consisting of M fixed number of time slots. Each frame length is equal to the length of the voice encoder frame and consists of three parts: a voice, a data, and a voice setup compartment. The voice compartment carries voice packets, one in each time slot, and has a movable boundary limiting its size to at most B slots.

[1]The discussion here is specific of a time-division multiple access network, but it is straightforward to extend to other multiple access techniques, for example, when the concept of time slots is replaced by radio channels.

The data compartment carries data packets, one in each time slot, and has a size equal to the number of slots left unused by the other compartments. The voice setup compartment is only used by calls intending to initially enter the system.

Speech is basically a variable rate source. For a given fidelity criterion, at any time, the rate of speech source depends on the level of voice activity. We assume that the system employs an L-state voice encoder with one distinct rate associated with each state; for instance, the QCELP coder has four states and four rates [7]. From now on, we use the terms "encoder state" and "call state" interchangeably. We assume framing and timing parameters so that the voice encoder rate corresponds to an integer number of packets per frame. We denote by $x_l^{\max}$ the requested bandwidth in terms of the number of slots per frame for a call in state l. For instance, QCELP produces one of one, two, four, or eight packets per frame depending on the encoder state. If a new call meets the criteria imposed by the network admission control policy, it will be admitted and the network will allow sending packets to the base station for the duration of the call. Although this implies a commitment of network resources for the duration of the call, in order to perform an efficient statistical multiplexing, the amount of committed resources will change depending on the call and the network state. Furthermore, no commitment is given to the data traffic.

Because of the dynamic state change of each voice call, a mechanism for allocating bandwidth, measured as the number of time slots per frame, is needed. In each transmission period, each call transmits the packets generated in the previous frame along with the bandwidth requested to transmit the packets generated in the current frame. The overall result is that while calls undergo a fixed delay equal to one frame, SEAMA knows all the bandwidth requests necessary to control the network flow. Using a feedback channel, SEAMA assigns slots to each call based on the next states of all calls as well as the available network resources (total bandwidth). For most practical coders, this procedure causes a delay that is tolerable in two-way voice communication situations.

SEAMA controls network flow and admissions of a network section from a centralized position. In its flow control task, SEAMA determines the rate assignment among calls to avoid congestion. Congestion, or equivalently overflow, occurs when the total requested bandwidth exceeds the voice compartment capacity. Specifically, let N_t denote the number of ongoing calls in the tth frame, let $N_{l,t}$ be the number of ongoing calls in state l, each requesting $x_l^{\max}$ slots per frame. Then, overflow occurs when $\sum_{l=1}^{L} N_{l,t} x_l^{\max} > B$. Because SEAMA knows the bandwidth requested by each call one transmission period earlier, it can detect the occurrence of congestion and resolve it. To resolve overflow while providing the best QoS for the voice traffic, voice calls use an encoder producing an embedded bit stream within each state. SEAMA's flow control mechanism exploits the hierarchical structure of the embedded encoder bit stream by selectively dropping low-significance packets to avoid overflow. An embedded source encoder produces a sequence of source descriptions with the property that each source description, except the first, may be decomposed into the prior source description and incremental descriptions. By decoding this sequence, the decoder can obtain a sequence of source reconstructions with decreasing expected distortions. It was shown in [6] that, to optimally resolve congestion by minimizing an increase in average distortion, the rates of all calls in the same state should be either the same or maximum one slot apart. Even more, [6] presented a greedy but optimal algorithm that SEAMA uses to resolve the overflow problem and to determine the bandwidth assignment to each call. Figure 1 summarizes the main flow control operations carried on by SEAMA for the voice subsection.

SEAMA also implements an admission control policy that determines the maximum admissible number of calls, hereafter denoted by $N_{\max}$. The policy accounts for the two interrelated facts that the overflow probability increases as more calls are admitted and that the overflow resolution increases the average distortion per call. An appropriate solution for this policy is to choose the maximum number of voice calls, so that the peak-load average distortion is kept below a threshold d, where the peak-load distortion, $\bar{E}[D]$, is defined as the average distortion per call when the number of calls in the network is maximum, $\bar{E}[D] = E[D(N) \mid N = N_{\max}]$. Here $D(N)$ is the average distortion per call normalized to its minimum value (i.e., the minimum value of D is 1). Note that we have dropped from the notation the time reference. This is because, without loss of generality, we will consider in the sequel the network state at some generic time. In the notation we now emphasize the dependence of the distortion on the random number of users present in the system N.

3. SLOW MOVABLE-BOUNDARY SEAMA DESIGN

As presented in [6] SEAMA implemented an FMB between voice and data sections. Specifically the boundary was set at every frame based on the state of each call by doing $B_F = \min[\sum_{l=1}^{L} n_l x_l^{\max}, B]$, where n_l is the number of calls in state l and B is the maximum number of slots allocated to the voice compartment. Because of the frequent boundary adaptation (typically tens of times per second if using practical coders), we call this scheme FMB-SEAMA.

In SMB-SEAMA the boundary changes slowly based on the number of voice calls in the network. Because the number of calls change roughly every few seconds, the frequency with which the boundary is changed in the SMB scheme is, depending on the voice subsection load, approximately three orders of magnitude smaller than the adaptation frequency in the FMB scheme. Given n ongoing calls in the system, the boundary is obtained such that the average distortion, conditioned on the number of calls in the network N, does not exceed a limit d, that is, $E[D(N) \mid N = n] \leq d$. Let $q_1 \cdots q_L$ be the occurrence probability of each of the L encoder states.

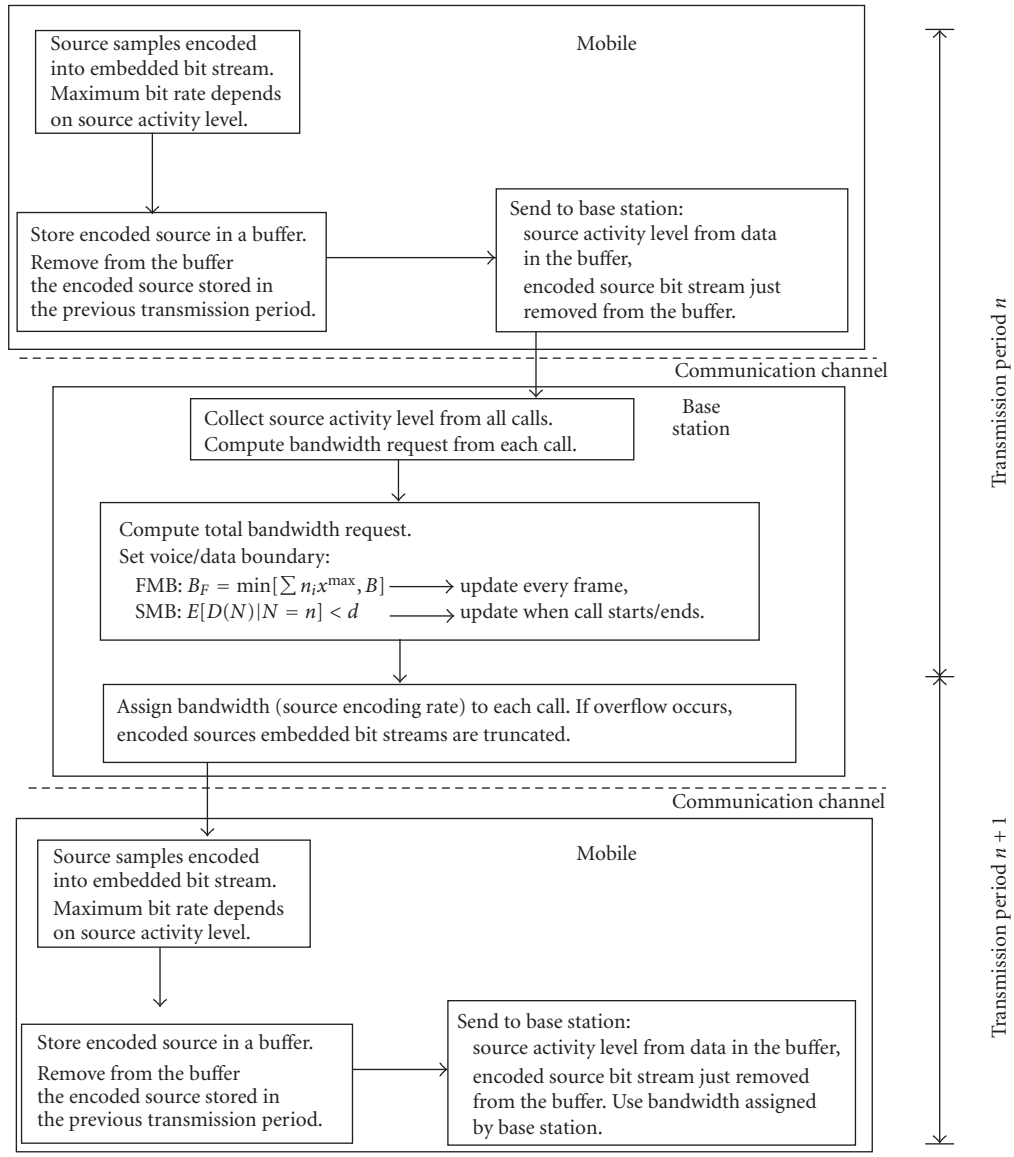

Figure 1: SEAMA's flow control operation.

Then, in a network supporting n calls we have

$$E[D(N) \mid N = n] = \sum_{n_1+\cdots+n_L=n} \binom{n}{n_1 \cdots n_L} q_1^{n_1} \cdots q_L^{n_L} D(n_1, \ldots, n_L), \tag{1}$$

where $D(n_1, \ldots, n_L)$ is the optimum average normalized distortion per call resulting from SEAMA flow control operation, which assigns rates among calls as described in [6, Section 2].

In our design we use the high-rate approximation for the distortion-rate encoder, given by $f_l(x) = \alpha_l 2^{2kx}$, $x \le x_l^{\max}$, where k is a scaling factor converting from bits per second (bps) to number of slots and α_l is a coder-dependent parameter [8]. Assuming that, when operating at maximum encoding rate, the average distortions in each state are all the same and equal to a constant δ, the encoder normalized distortion-rate performance in state l is $f_l(x)/\delta = 2^{2k(x_l^{\max}-x)}$. In the absence of rate control, the average normalized distortion per call is $(1/n)\sum_{l=1}^{L} n_l 2^{2k(x_l^{\max}-x)}$. However, in the presence of an overflow SEAMA optimally controls each call voice encoding rate. It was shown in [6] that, following this optimal rate adaptation,

$$D(n_1, \ldots, n_L) = \left(\prod_{l=1}^{L} 2^{2k(n_l/n)x_l^{\max}} \right) 2^{-2k(B/n)}, \tag{2}$$

where B in (2), when referred to FMB-SEAMA, is the maximum number of slots allocated to the voice compartment.

In SMB-SEAMA, this boundary changes based on the number of calls present in the system. Denoting by $B_S(n)$ the boundary setting in SMB-SEAMA when there are n users and combining (1) and (2),

$$E[D(N) \mid N = n] = (n!2^{-2k(B_S(n)/n)}) \sum_{n_1+\cdots+n_L=n} \prod_{l=1}^{L} \left(\frac{q_l^{n_l} 2^{2kx_l^{\max} n_l/n}}{n_l!} \right). \quad (3)$$

The problem of designing the voice/data boundary is, then, the one of finding $B_S(n)$ such that $E[D(N) \mid N = n] \leq d$. This leads to the SMB design formula

$$B_S(n) = \left\lceil \frac{n}{2k} \log_2 \left(\frac{n! \sum_{n_1+\cdots+n_L=n} \prod_{l=1}^{L} (q_l^{n_l} 2^{2kx_l^{\max} n_l/n}/n_l!)}{d} \right) \right\rceil. \quad (4)$$

Note that, because of the admission control policy which sets $N_{\max}$ considering B and $E[D|N = N_{\max}] \leq d$, we have that $B_S(N_{\max}) = B$.

4. SLOW MOVABLE-BOUNDARY SEAMA ANALYSIS

Because the movable voice/data boundary is the main tool used here to integrate voice and data, its adaptation affects both voice and data traffic within the same frame. In this section we analyze the movable-boundary setting and both the voice and data subsystem performance.

4.1. Movable-boundary setting

We assume that the number of calls present in the system, n, is fixed and large, and consider the average normalized distortion $D(n_1, \ldots, n_L)$ in the presence of an overflow, from (2),

$$D\left(n = \sum_{l=1}^{L} n_l\right) = D(n_1, \ldots, n_L) = 2^{(2k/n)(\sum_{l=1}^{L} n_l x_l^{\max} - B(n))} = 2^{(2k/n)(\sum_{i=1}^{n} x_i^{\max} - B(n))} = 2^{(2k/n)(S(n) - B(n))}, \quad (5)$$

where we have defined $S(n) \triangleq \sum_{i=1}^{n} x_i^{\max}$. Let μ_X be the average number of slots requested by each call (i.e., $\mu_X = \sum_l q_l x_l^{\max}$) and σ_X^2 the variance. Using the assumption that the number of users is large, and resorting to the law of large numbers [9], we can say that $S(n)/n \approx \mu_X$ with high probability. Therefore,

$$D(n) \approx 2^{2k(\mu_X - B(n)/n)}. \quad (6)$$

Using (6) in (1) and considering the design condition $E[D(N) \mid N = n] \leq d$, we have

$$d \approx \sum_{n_1+\cdots+n_L=n} \binom{n}{n_1 \cdots n_L} q_1^{n_1} \cdots q_L^{n_L} 2^{2k(\mu_X - B(n)/n)} \approx 2^{2k(\mu_X - B(n)/n)} \sum_{n_1+\cdots+n_L=n} \binom{n}{n_1 \cdots n_L} q_1^{n_1} \cdots q_L^{n_L}. \quad (7)$$

From here, since the sum adds up to 1, we get

$$\log_2 d \approx 2k\left(\mu_X - \frac{B(n)}{n}\right). \quad (8)$$

Through algebraic operations, this equation leads to

$$B(n) \approx n\left(\mu_X - \frac{1}{2k} \log_2 d\right). \quad (9)$$

This result allows us to derive the following lemma.

Lemma 1. *Assuming that the fixed number of voice calls is large, then* $B_S(n) \approx \mu_X n$.

Proof. The proof follows from considering that under practical operating conditions, d is a number close to one and k is larger than 1. Then $\mu_X \gg (\log_2 d)/(2k)$. □

From Lemma 1, we can derive the important conclusion that SMB-SEAMA is a highly efficient MAC protocol. To see this, consider that in a circuit-switched system, the number of slots permanently assigned to each call equals the maximum bandwidth request. Statistical multiplexers assign less time slots per call than the number assigned in a circuit-switched system because they take advantage of the source statistics. This more efficient time slot assignment comes as a tradeoff with the probability of having to drop some packets because of a lack of time slots. For example, in PRMA [3], the number of time slots assigned per call is determined by a limit on the packet drop probability. This tradeoff is translated on an average number of slots assigned per call that is less than the number assigned in a circuit-switched system but more than the average number of slots requested by each call, μ_X. Lemma 1 shows that in SMB-SEAMA this assignment, commonly known as *effective bandwidth*, is very close to the average number of slots requested by each call, that is, μ_X, which is a highly efficient result. This conclusion is illustrated in Figure 2, which shows the probability density function (pdf) of the average rate request, $S(n)/n$, when there is a large number of users in the system. In the figure we used the central limit theorem (CLT) to approach this distribution to a Gaussian distribution. Alongside with this distribution, we also exemplify the average rate assignment for the multiplexing cases we have discussed. Note how the SMB-SEAMA assigns the smallest number of slots per call, followed by a statistical multiplexer (e.g., PRMA) and a circuit-switched system.

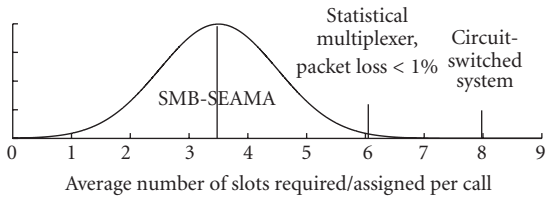

Figure 2: Average bandwidth request, $S(n)/n$, and the corresponding assignment for different multiplexing techniques.

Figure 3 summarizes the design and analysis results for $B_S(n)$ following both the design equation (4) and Lemma 1. We calculated $B_S(n)$ using (4) for d equal to 1.1 and 1.25, that is, 10% and 25% additional average normalized distortion compared to the one where all calls transmit at full rate. In the case of Lemma 1, we set $d = 1.25$. We choose as voice encoder a QCELP-like encoder developed at the University of Maryland's Communications and Signal Processing Laboratory (CSPL). This encoder is similar in structure to QCELP, being multistate with different rates associated with each state. It differs from QCELP in that the output stream is embedded, which allows for the flow control protocol to adapt encoding rate by selectively dropping source packets. Because of this property we named the encoder embedded QCELP. To calculate $B_S(n)$, we measured the encoder-dependent parameters as being $L = 4$, $x_1^{\max} = 1$, $x_2^{\max} = 2$, $x_3^{\max} = 4$, $x_4^{\max} = 8$, $q_1 = 0.585$, $q_2 = 0.035$, $q_3 = 0.050$, and $q_4 = 0.330$. According to our tests on the embedded-QCELP encoder, we have found that the impact on perceptual quality when allowing 10% or even 25% additional average distortion is almost negligible. Note that the design results show a very small dependence on the design value chosen for d. This is because the values chosen for d are relatively small so that the perceived quality degradation is kept negligible. Note that this observation was expected from Lemma 1 and its proof. Figure 3 also shows the values for $B_S(n)$ obtained using Lemma 1. These results clearly shows that the approximation in Lemma 1 is very tight and that the protocol is highly efficient.

4.2. Voice subsystem

It is clear from our study so far that, when using the SMB, calls are going to be operating with an average distortion equal to the target d. Nevertheless, the instantaneous distortions per call change following the total bandwidth request. Equations (2) and (5) show the average normalized distortion $D(n_1, \ldots, n_L)$ in the presence of an overflow. Clearly, when there is no overflow, calls will be carried on with no packets dropping, thus $D(n_1, \ldots, n_L) = 1$. We can combine these two operational conditions into a single equation for $D(n_1, \ldots, n_L)$. From (5)

$$D(n_1, \ldots, n_L) = 2^{(2k/n)\{\sum_{l=1}^{L} n_l x_l^{\max} - B(n)\}^+}, \tag{10}$$

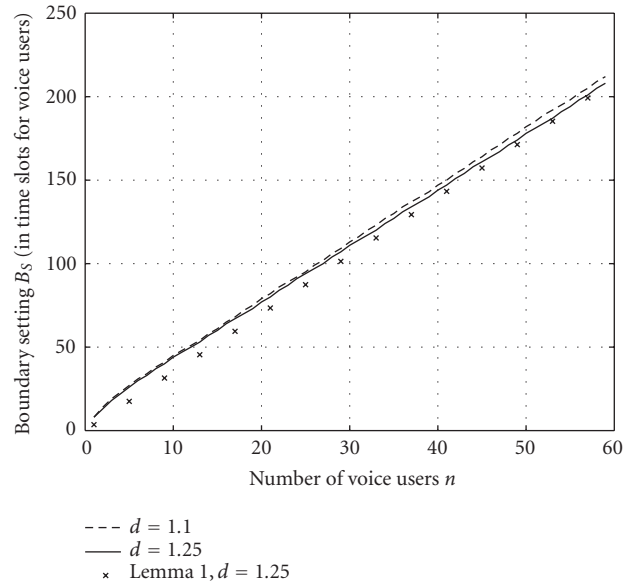

Figure 3: Voice/data movable boundary $B_S(n)$, measured as the number of slots reserved for voice traffic in a frame, as a function of the number of calls in the network.

where $\{x\}^+ \triangleq \max[0, x]$. Therefore,

$$\begin{aligned} D(n) &= D(n_1, \ldots, n_L) \\ &= 2^{(2k/n)\{\sum_{i=1}^{n} x_i^{\max} - B(n)\}^+} \\ &= 2^{(2k/n)\{S(n) - B(n)\}^+}. \end{aligned} \tag{11}$$

Note that the domain of $D(n)$ is $[1, \infty]$ because $D(n)$ is a measure of a normalized distortion. Equation (11) shows that the case $D(n) = 1$ (when $S(n) \leq B(n)$) needs to be considered separately from the case $D(n) > 1$ (when $S(n) > B(n)$). For the case $D(n) = 1$ we have $P[D(n) = 1] = P[S(n) \leq B(n)]$. Assuming that the number of users is fixed and large, we can apply the CLT to approximate the distribution of $S(n)/n$ as

$$\frac{S(n)}{n} \longrightarrow Z_n \sim \mathcal{N}\left(\mu_X, \frac{\sigma_X^2}{n}\right) \quad \text{in distribution.} \tag{12}$$

Then, using Lemma 1,

$$P[D(n) = 1] \approx 1 - Q\left(\frac{B(n) - n\mu_X}{\sigma_X \sqrt{n}}\right) \approx \frac{1}{2}, \tag{13}$$

where

$$Q(\theta) \triangleq \frac{1}{\sqrt{2\pi}} \int_{\theta}^{\infty} e^{v^2/2} dv. \tag{14}$$

The range of values where $D(n) > 1$ corresponds to the case when $D(n) = 2^{(2k/n)(S(n) - B(n))}$ in (11), that is,

when $S(n) > B(n)$. Over this range of values, the pdf of $D(n)$, $f_{D(n)}(\gamma)$, can be obtained through $f_{D(n)}(\gamma) = (d/d\gamma)P[D(n) \le \gamma]$. With

$$\begin{aligned} P[D(n) \le \gamma] &= \frac{1}{2} + P\left[2^{(2k/n)(S(n)-B(n))} \le \gamma\right] \\ &= P\left[S(n) \le B(n) + \frac{n}{2k}\log_2 \gamma\right] \\ &= 1 - Q\left(\frac{B(n) + (n/2k)\log_2 \gamma - n\mu_X}{\sigma_X\sqrt{n}}\right) \\ &\approx 1 - Q\left(\frac{(n/2k)\log_2 \gamma}{\sigma_X\sqrt{n}}\right), \end{aligned} \tag{15}$$

we have

$$\begin{aligned} \frac{d}{d\gamma}P[D(n) \le \gamma] &\approx \frac{d}{d\gamma}\left(1 - Q\left(\frac{\sqrt{n}\log_2 \gamma}{2k\sigma_X}\right)\right) \\ &= -\frac{d}{d\gamma}\int_{\sqrt{n}\log_2 \gamma/2k\sigma_X}^{\infty} \frac{e^{-v^2/2}}{\sqrt{2\pi}}dv \\ &= \frac{\sqrt{n}}{2k\sigma_X \gamma \ln 2}\frac{e^{-(\sqrt{n}\ln \gamma/2\sqrt{2}k\sigma_X \ln 2)^2}}{\sqrt{2\pi}}. \end{aligned} \tag{16}$$

Combining (13) and (16), the pdf of $D(n)$, $f_{D(n)}$, is

$$\begin{aligned} f_{D(n)}(\gamma) \approx{}& \frac{1}{2}\delta(\gamma - 1) \\ &+ \frac{\sqrt{n}}{2k\sigma_X \gamma \ln 2}\frac{e^{-(\sqrt{n}\ln \gamma/2\sqrt{2}k\sigma_X \ln 2)^2}}{\sqrt{2\pi}}, \quad \gamma \in [1, \infty], \end{aligned} \tag{17}$$

where $\delta(x)$ is Dirac's delta function.

Figure 4 illustrates this result when $d = 1.25$. In the figure we include the analytical function from (17) as well as the empirical result obtained from simulation using the embedded-QCELP encoder as described in Section 4.1. Note that even though in the process of developing (17), we did some simplifying assumptions, the result matches very closely the empirical observations. Also, note that there is a nonzero probability that distortion may exceed the acceptable range. Nevertheless, this does not contradicts our claim that $d = 1.25$ is an acceptable value. The reason for this is that, because of their relatively low probability of occurrence, the system operates under high distortion for short periods of time and close to the average distortion d most of the time. In terms of subjective perception of the received speech quality, the high distortion values become insignificant because of their short duration.

4.3. Data subsystem

We have already emphasized the fact that, because the boundary is changed based on the number of active voice calls, for the data subsystem the voice subsystem appears as being circuit switched. Our goal in this section is to analyze

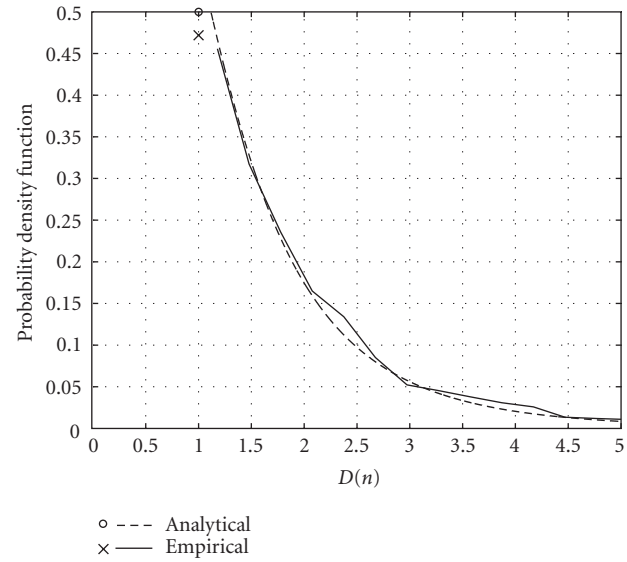

Figure 4: The probability density function of the average normalized distortion per voice call $D(n)$.

the performance of the data subsystem in terms of the average system delay. For this purpose we assume that the data traffic consists of packets arriving following a Poisson arrival process with rate λ_d. Each packet is transmitted in one time slot. Those packets that cannot be transmitted because at the time of transmission all time slots in the data subsection are occupied by other data packets wait in a queue of infinite length and first-in-first-out (FIFO) service discipline. We will show next that the behavior of the data subsystem is the one of a variable number of servers (those time slots in the frame unoccupied by voice calls), each with constant service time (equal to the frame transmission time).

Let N_t be the number of voice calls at time t, B_t the number of slots assigned to the voice subsystem at time t (movable-boundary setting at time t), G_t the number of backlogged data packets at time t, and d_t the number of data packets arriving at time t. We assume that packets arriving during the frame corresponding to time t are put in the waiting queue until at least the beginning of the next frame. Therefore, at time t we have

$$G_t = \{G_{t-1} - (M - B_t)\}^+ + d_t. \tag{18}$$

From (18),

$$\begin{aligned} P[G_t = i] &= \sum_{j=0}^{\infty}\sum_{b=0}^{B} P[G_t = i,\ B_t = b,\ G_{t-1} = j] \\ &= \sum_{j=0}^{\infty}\sum_{b=0}^{B} P[G_{t-1} = j]P[B_t = b \mid G_{t-1} = j] \\ &\qquad \times P[G_t = i \mid G_{t-1} = j,\ B_t = b]. \end{aligned} \tag{19}$$

Let $P_i \triangleq P[G_t = i]$ and $\hat{p}_b \triangleq P[B_t = b]$, $b = 0, 1, 2, \ldots, B$.

Assuming that the data packet backlog process is in the steady state and using the fact that the movable-boundary setting is independent of the data packet backlog process and using (18),

$$\begin{aligned} P_i &= \sum_{j=0}^{\infty}\sum_{b=0}^{B} P[G_{t-1}=j]P[B_t=b] \\ &\qquad \times P\left[\{G_{t-1}-(M-B_t)\}^+ \right. \\ &\qquad\qquad \left. + d_t = i \mid G_{t-1}=j,\ B_t=b\right] \\ &= \sum_{j=0}^{\infty}\sum_{b=0}^{B} \hat{p}_b P_j P[\{j+b-M\}^+ + d_t = i] \\ &= \sum_{b=0}^{B} \hat{p}_b \left\{ \sum_{j=0}^{\infty} P_j P[d_t = i - \{j+b-M\}^+] \right\}. \end{aligned} \tag{20}$$

Therefore,

$$P_0 = \sum_{b=0}^{B} \hat{p}_b \left\{ p_0 \sum_{j=0}^{M-b} P_j \right\}, \tag{21}$$

and for $i = 1, 2, \ldots, \infty$, with $p_k \triangleq P[d_t = k]$,

$$\begin{aligned} P_i &= \sum_{b=0}^{B} \hat{p}_b \left\{ p_i \sum_{j=0}^{M-b} P_j \right\} + \sum_{b=0}^{B} \hat{p}_b \left\{ \sum_{j=M-b+1}^{M-b+i} p_{i+M-j-b} P_j \right\} \\ &= \sum_{b=0}^{B} \hat{p}_b \left\{ p_i \sum_{j=0}^{M-b} P_j \right\} + \sum_{b=0}^{B} \hat{p}_b \left\{ \sum_{j=1}^{i} p_{i-j} P_{j+M-b} \right\}. \end{aligned} \tag{22}$$

Let $g_G(z) \triangleq \sum_{i=0}^{\infty} P_i z^i$ be the probability generating function of the data backlog process. Assuming that the voice call traffic is Poisson (λ) with exponential (η) holding times [10] and that the number of ongoing calls, N, is limited to $N_{\max}$, then Appendix A.1 shows that

$$g_G(z) = \frac{H(z) - z^M Q}{C \sum_{k=0}^{N_{\max}} (\rho_V^k / k!) z^{B(k)} - z^M e^{\lambda_d (1-z)}}, \tag{23}$$

where $C = (\sum_{k=0}^{N_{\max}} \rho_V^k / k!)^{-1}$, ρ_V is the voice subsection load, $\rho_V = \lambda/\eta$, λ_d is the data packets average arrival rate,

$$\begin{aligned} Q &\triangleq \sum_{k=0}^{N_{\max}} \check{p}_k \left\{ \sum_{j=0}^{M-B(k)} P_j \right\}, \\ H(z) &\triangleq \sum_{k=0}^{N_{\max}} \check{p}_k z^k \left\{ \sum_{j=0}^{j=M-B(k)} z^j P_j \right\}. \end{aligned} \tag{24}$$

From (23), we show in Appendix A.2 that the data backlog process probability generating function can be written as

$$g_G(z) = \frac{(M - \lambda_d - E[B_t])(1-z)}{C \sum_{k=0}^{N_{\max}} (\rho_V^k / k!) z^{B(k)} - z^M e^{\lambda_d (1-z)}} \prod_{r=1}^{M-1} \frac{z - z_r}{1 - z_r}, \tag{25}$$

where z_r are the zeroes of the denominator in (23).

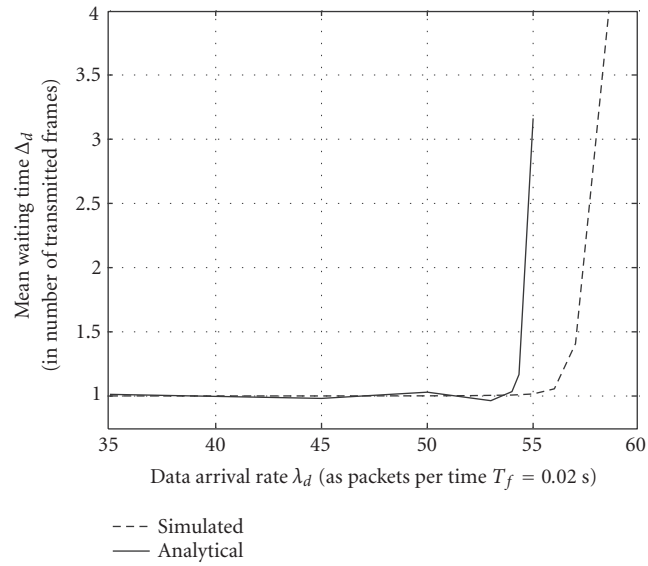

Figure 5: Mean waiting time obtained using (27).

Using this result and the well-known property $E[G_t] = \lim_{z\to 1} dg_G(z)/dz$, Appendix B shows that the mean number of backlogged data packets is

$$E[G_t] = \sum_{r=1}^{M-1} \frac{1}{1-z_r} + \frac{M - (M-\lambda_d)^2 + E[B_t^2] - E[B_t]}{2(M - \lambda_d - E[B_t])}. \tag{26}$$

Finally, using Little's law, the mean data packet delay, Δ_d, is

$$\Delta_d = \left[\sum_{r=1}^{M-1} \frac{1}{1-z_r} + \frac{M - (M-\lambda_d)^2 + E[B_t^2] - E[B_t]}{2(M - \lambda_d - E[B_t])} \right] \frac{1}{\lambda_d}. \tag{27}$$

This result has the form of a modified version of the formula for the mean waiting time of a system with Poisson input and multiple servers with constant service time [11]. Of course, the differences are due to the fact that the voice/data boundary (in effect the number of servers) changes over time based on the number of users present in the system. This process that changes the number of servers (i.e., the voice/data boundary setting) is represented by its probability generating function. As an application example, Figure 5 shows the mean waiting time obtained through (27) for a system using the same embedded-QCELP decoder described in Section 4.1, the total number of slots $M = 150$, maximum number of voice calls $N_{\max} = 27$, and $\rho_V = 20$. The figure also includes, for comparison purposes, empirical result obtained from simulation using the embedded-QCELP encoder as described in Section 4.1. Both results match each other closely. The difference between them, about 3% at most, is for the most part due to the sensibility of the solution to inaccuracies in calculating the poles z_r and due to the slow convergence in finding them. Therefore, (27) can be used to

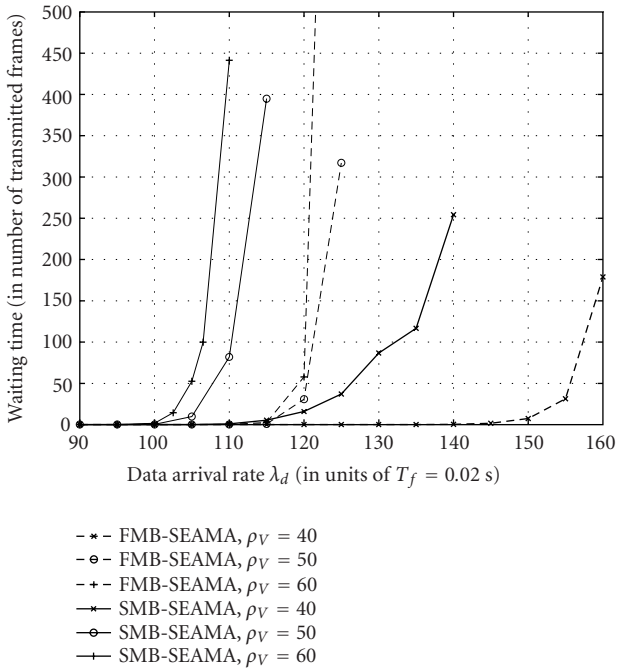

Figure 6: Average waiting time as a function of data packets arrival rate (λ_d) with voice subsection load, ρ_V, as a parameter. Normalized distortion threshold equals 1.1.

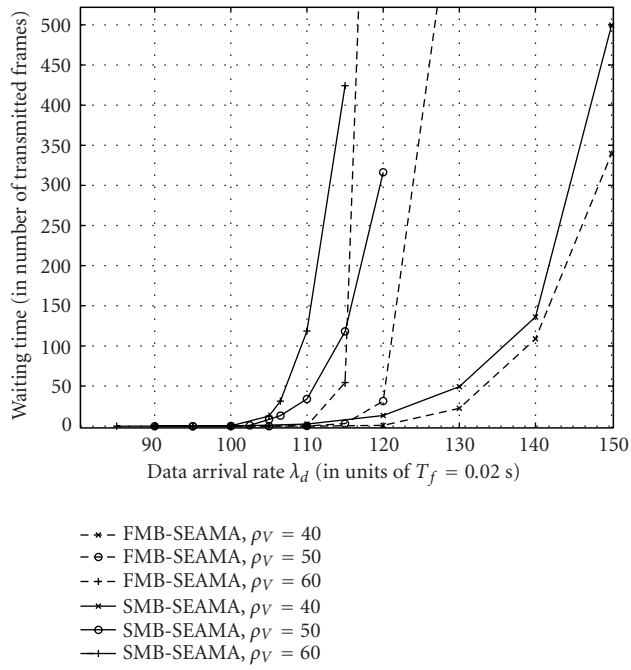

Figure 7: Average waiting time as a function of data packets arrival rate (λ_d) with voice subsection load, ρ_V, as a parameter. Normalized distortion threshold equals 1.25.

estimate the mean data packet delay. Because (27) follows from the assumption of a system in steady state, it is also important to note that this result is valid up to the operating point when the queuing system becomes instable and the mean waiting time grows rapidly. Finally we note that in (25) we could have used Lemma 1 to do the approximation $B_t(n) \approx \mu_X n$. Also, assuming ergodicity of all the processes involved, the first- and second-order statistics $E[B_t]$ and $E[B_t^2]$ can be approximately calculated as

$$E[B_t] \approx E[\mu_X n] = \mu_X \frac{\sum_{k=0}^{N_{\max}} k(\rho_V^k/k!)}{\sum_{k=0}^{N_{\max}} (\rho_V^k/k!)},$$
$$E[B_t^2] \approx E[(\mu_X n)^2] = \mu_X^2 \frac{\sum_{k=0}^{N_{\max}} k^2(\rho_V^k/k!)}{\sum_{k=0}^{N_{\max}} (\rho_V^k/k!)}. \quad (28)$$

5. PERFORMANCE SIMULATION

In this section, we present simulation results aimed at providing insight into the performance of the new design combining a slow movable voice/data boundary and selective voice packet dropping from an embedded stream. We focus on simulations aimed at evaluating the impact on the data subsection as compared to other solutions. For this purpose we used the same setup as in [6]. The TDMA frame size is assumed to be $T_f = 200$ milliseconds. A frame consists of $M = 300$ time slots, with a maximum of $B = 200$ allocated to voice calls. For FMB-SEAMA, using $E[D|N = N_{\max}] \le d$ as an admission control condition, from (3) with $n = N_{\max}$ and using the fact that $B_S(N_{\max}) = B = 200$, we found that $N_{\max} = 55$ for $d = 1.1$ and $N_{\max} = 57$ for $d = 1.25$ (this can also be seen in Figure 3). As discussed, these values of distortion were chosen because our test have shown that they correspond to a perceptually negligible distortion.

In simulations, we assumed a Poisson arrival process (i.e., exponential interarrival time) with rate λ for voice calls with the random calls duration following an exponential distribution with mean $1/\eta$. Three cases of voice subsection load were considered with $\rho_V = \lambda/\eta$ equal to 40, 50, and 60 and with $1/\eta = 3$ minutes [12] in all cases. The voice encoder used was the embedded QCELP described in Section 3.

For the data subsection we assumed also that packets arrive following a Poisson process with rate λ_d. Each data packet has size equal to one slot, thus each is serviced during the duration of one slot. We assume that packets may be transmitted in the same frame where they arrive if possible.

We first compared both SMB and FMB schemes by measuring the maximum data arrival rate that can be supported by each network configuration before the data subsection of the network is overflowed. Simulations were performed using Monte Carlo method with a simulation time long enough so as to guarantee the statistical confidence in the results. We measured the average queuing delay for both FMB-SEAMA and SMB-SEAMA as a function of the data arrival rate under different voice network loads and by allowing either 10 or 25 percent additional average distortion per call ($d = 1.1$ or $d = 1.25$). These results are shown in Figures 6 and 7. To consistently measure the maximum data arrival rate that can be supported by each network configuration before data section

Table 1: Data subsection comparison between FMB and SMB.

d	ρ_V	λ_d FMB-SEAMA	λ_d SMB-SEAMA	Difference	Relative difference
1.10	40	155	126	29	0.19
1.10	50	120	108	12	0.10
1.10	60	120	115	15	0.13
1.25	40	134	130	4	0.03
1.25	50	120	111	9	0.08
1.25	60	115	108	7	0.06
1.50	40	135	130	5	0.04
1.50	50	116	108	8	0.07
1.50	60	111	105	6	0.05

overflow, we estimated the overflow point to roughly correspond to a time in queue equal to 50 frames in all cases. Because steady-state behavior of the system cannot be assured for the measurements of interest in this case, we did not use (27). Results are summarized in Table 1. We can see that the downsizing of reducing complexity by using an SMB scheme is some data subsection performance reduction. This reduction is noticeable in the case when $d = 1.10$. Nevertheless, this case corresponds to an overly restrictive design. We have noticed that a value of $d = 1.25$ is completely acceptable from the subjective performance point of view. In this case, the degradation in performance is small (ranging from 3% to 8%), especially when considering that the boundary is updated at a frequency three orders of magnitude smaller. It is clear from these results that the design should consider performance, complexity, and distortion as three interrelated variables. The observation that the choice of a larger d attenuates the performance reduction in the data subsection was confirmed by measuring the performance when $d = 1.50$. These results are also included in Table 1.

It is important to consider that a larger, yet still acceptable, value of distortion threshold is not only desirable in view of these results but also because it maximizes the performance improvement of SEAMA when compared to other multiple access protocols, such as PRMA [3, 4, 6]. Due to a number of key differences between PRMA and SEAMA (both SMB and FMB schemes), it is not possible to compare them using the same setup as described above. Perhaps the most important difference is that PRMA uses a two-state vocoder that transmits at full rate for speech periods and does not transmit at all during silence. Then, in an overflow situation, while SEAMA selectively drops a portion of packets, PRMA drops all of them, effectively silencing an active user. Because of this, PRMA is set to operate at a low overflow probability (typically 1%). In SEAMA, overflow configuration is based on the distortion threshold. Also, PRMA differs from SEAMA in the access method. Since in PRMA active users contend for access to the channel in every silence-to-talk spurt transition it is possible that users may be silenced at the beginning of a talk spurt if a contention occurs. In summary, the overall effect of these differences is that fair comparison between SEAMA and PRMA can only be drawn in conditions where subjective quality of speech is similar. To achieve this, both access methods need to be compared at a fixed number of users. In the present case, we fixed the number of voice users to $n = 36$. For PRMA, a 1% packet dropping probability condition determined a maximum number of voice time slots $B_p = 176$. Furthermore, we assumed that this was also the total number of time slots in a frame. Having set up the simulation parameters from PRMA, we proceeded to test SEAMA searching for the value of B where the perceived quality is similar to PRMA. This value was found equal to $B_s = 117$. Note that in this setup we are implicitly fixing for SEAMA the maximum number of users as well as the corresponding boundary. This makes both FMB-SEAMA and SMB-SEAMA equivalent. Comparison between SEAMA and PRMA was done using the same criteria as above, that is, we measured the maximum data arrival rate that can be supported before data subsection overflow. The results are shown in Figure 8. Here we can see that PRMA supports approximately 13% less data arrival rate.

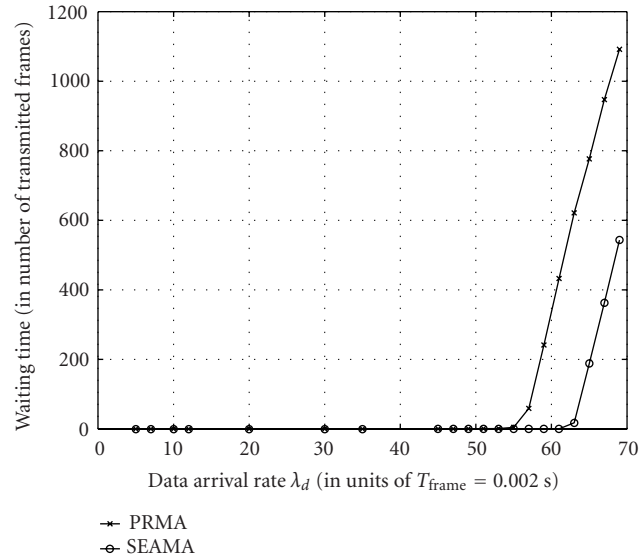

Figure 8: Average waiting time versus arrival rate (λ_d) for data packets for both PRMA and SEAMA.

Combining all the simulations results we can conclude that SMB-SEAMA presents an acceptable reduction in performance, considering the reduction in complexity, when compared to FMB-SEAMA. Even more, from these results we can also infer that SMB-SEAMA should still outperform PRMA.

6. CONCLUSIONS

In this paper, we have presented, designed, analyzed, and evaluated a reduced complexity variation to the source encoding assisted multiple access (SEAMA) protocol. The variation, denoted as SMB-SEAMA, uses at the application layer the same embedded and multistate voice encoder used in FMB-SEAMA. The new scheme, instead of setting the voice/data boundary based on the frame-by-frame bandwidth demand, sets the boundary based on the number of active voice calls in the system and a maximum average normalized distortion threshold. This results in a protocol that, at the network layer, is packet switched for both voice and data; however, from data traffic point of view, the voice subsection looks as a simple circuit-switched network.

We have also presented mathematical analysis that develops a model to describe the boundary setting and both the voice and data queuing subsystems behavior. These results allowed us to find a tight approximation for the boundary setting that shows that SMB-SEAMA is a very efficient MAC protocol, allocating a number of time slots to voice calls very close to the one necessary for all speech users to communicate at the average encoding rate. In addition to this, the result for the data subsection models the behavior of a multiserver queuing system with fixed service time and infinite waiting queue where the number of servers changes over time following some random process (a truncated Poisson in our case).

In the design, we have used average distortion values that have been shown in informal tests to have an almost negligible impact on perceptual quality. Simulations results using an acceptable distortion threshold show that the SMB scheme does not significantly affect performance (less than 8% in maximum acceptable data arrival rate). Even more, simulations also show that SMB-SEAMA could still outperform pure packet-switched protocols such as PRMA (accepts 12% more data arrival rate). The overall result is then a highly efficient, low-complexity MAC protocol with an SMB that provides a performance comparable with SEAMA.

APPENDICES

A. DERIVATION OF EXPRESSIONS FOR THE PROBABILITY GENERATING FUNCTION OF THE DATA BACKLOG PROCESS

A.1. Probability generating function of the data backlog process

In this appendix, we intend to show that the data backlog process probability generating function is as shown in (23).

Let $g_G(z) \triangleq \sum_{i=0}^{\infty} P_i z^i$, $g_B(z) \triangleq \sum_{b=0}^{B} \hat{p}_b z^b$, and $g_d(z) \triangleq \sum_{i=0}^{\infty} p_i z^i$ be the probability generating function of the data backlog, the boundary setting, and the data arrival processes, respectively. Using (21) and (22) we have

$$\begin{aligned}
g_G(z) &= \sum_{b=0}^{B} \hat{p}_b \left\{ p_0 \sum_{j=0}^{M-b} P_j \right\} + \sum_{b=0}^{B} \hat{p}_b \left\{ \sum_{i=1}^{\infty} z^i p_i \sum_{j=0}^{M-b} P_j \right\} \\
&\quad + \sum_{b=0}^{B} \hat{p}_b \left\{ \sum_{i=1}^{\infty} \sum_{j=1}^{i} z^i p_{i-j} P_{j+M-b} \right\} \\
&= \sum_{b=0}^{B} \hat{p}_b \left\{ \left(\sum_{i=0}^{\infty} z^i p_i \right) \left(\sum_{j=0}^{M-b} P_j \right) \right\} \\
&\quad + \sum_{b=0}^{B} \hat{p}_b \left\{ \sum_{j=1}^{\infty} \sum_{i=j}^{\infty} z^i p_{i-j} P_{j+M-b} \right\} \\
&= \sum_{b=0}^{B} \hat{p}_b \left\{ g_d(z) \sum_{j=0}^{M-b} P_j \right\} \\
&\quad + \sum_{b=0}^{B} \hat{p}_b \left\{ \sum_{j=1}^{\infty} z^j P_{j+M-b} \left(\sum_{i=j}^{\infty} z^{i-j} p_{i-j} \right) \right\} \\
&= g_d(z) \sum_{b=0}^{B} \hat{p}_b \left\{ \sum_{j=0}^{M-b} P_j \right\} \\
&\quad + g_d(z) \sum_{b=0}^{B} \hat{p}_b z^{-M+b} \left\{ \sum_{j=1}^{\infty} z^{j+M-b} P_{j+M-b} \right\} \\
&= g_d(z) \sum_{b=0}^{B} \hat{p}_b \left\{ \sum_{j=0}^{M-b} P_j \right\} \\
&\quad + g_d(z) \sum_{b=0}^{B} \hat{p}_b z^{-M+b} \left\{ \sum_{j=M-b+1}^{\infty} z^j P_j \right\} \\
&= g_d(z) \sum_{b=0}^{B} \hat{p}_b \left\{ \sum_{j=0}^{M-b} P_j \right\} \\
&\quad + g_d(z) \sum_{b=0}^{B} \hat{p}_b z^{-M+b} \left\{ \sum_{j=0}^{\infty} z^j P_j - \sum_{j=0}^{j=M-b} z^j P_j \right\} \\
&= g_d(z) \sum_{b=0}^{B} \hat{p}_b \left\{ \sum_{j=0}^{M-b} P_j \right\} \\
&\quad - g_d(z) \sum_{b=0}^{B} \hat{p}_b z^{-M+b} \left\{ \sum_{j=0}^{j=M-b} z^j P_j \right\} \\
&\quad + g_d(z) z^{-M} g_B(z) g_G(z).
\end{aligned} \tag{A.1}$$

We can define $Q \triangleq \sum_{b=0}^{B} \hat{p}_b \{ \sum_{j=0}^{M-b} P_j \}$ and $H(z) \triangleq \sum_{b=0}^{B} \hat{p}_b z^b \{ \sum_{j=0}^{j=M-b} z^j P_j \}$. Then,

$$g_G(z) = \frac{H(z) - z^M Q}{g_B(z) - z^M [g_d(z)]^{-1}}. \tag{A.2}$$

Since the data arrival is a Poisson process with average arrival rate λ_d, its probability generating function is given by, [9], $g_d(z) = e^{\lambda_d(z-1)}$. To find $g_B(z)$ we first note that $\hat{p}_{B(n)} \triangleq P[B_t = B(n)] = P[N_t = n]$. We also assume that the call traffic is Poisson (λ) with exponential (η) holding times [10]. The number of ongoing calls, N, is limited to $N_{\max}$, thus is a truncated-Poisson ($\rho_V, N_{\max}$) random variable where $\rho_V = \lambda/\eta$, that is, for $n = 0, 1, \ldots, N_{\max}$,

$$\check{p}_n \triangleq P[N = n] = \frac{\rho_V^n/n!}{\sum_{i=0}^{N_{\max}} \rho_V^i/i!}. \tag{A.3}$$

Therefore,

$$g_B(z) = \frac{\sum_{k=0}^{N_{\max}} (\rho_V^k/k!) z^{B(k)}}{\sum_{k=0}^{N_{\max}} \rho_V^k/k!}. \tag{A.4}$$

Denoting $C = (\sum_{k=0}^{N_{\max}} \rho_V^k/k!)^{-1}$, and with

$$\begin{aligned} Q &= \sum_{k=0}^{N_{\max}} \check{p}_k \left\{ \sum_{j=0}^{M-B(k)} P_j \right\}, \\ H(z) &= \sum_{k=0}^{N_{\max}} \check{p}_k z^k \left\{ \sum_{j=0}^{j=M-B(k)} z^j P_j \right\}, \end{aligned} \tag{A.5}$$

we finally get (23).

A.2. Alternate expression for the probability generating function of the data backlog process

Next, we can derive a more useful expression for $g_G(z)$ that does not explicitly depend on Q and $H(z)$. Note that the denominator of $g_G(z)$ in (23) has M zeros $z_r, r = 0, 1, \ldots, M-1$, which are the roots of

$$C \sum_{k=0}^{N_{\max}} \frac{\rho_V^k}{k!} z^{B(k)} - z^M e^{\lambda_d(1-z)} = 0. \tag{A.6}$$

Using the normalizing property for probability generating function $\lim_{z\to 1} g(z) = 1$, it is clear that one root is $z_0 = 1$. The rest of the roots can be obtained by setting in (A.6) $z_r = \gamma e^{-j\omega}$, with $j = \sqrt{-1}$, $C \sum_{k=0}^{N_{\max}} (\rho_V^k/k!) z^{B(k)} = \Gamma(z) e^{j\theta(z)}$, separating the real and imaginary parts to obtain the equations

$$\begin{aligned} \gamma &= \Gamma^{1/M} e^{\lambda_d(\gamma\cos\omega - 1)/M}, \\ \omega &= \frac{2\pi r + \theta + \gamma\lambda_d \sin\omega}{M}, \quad r = 1, 2, \ldots, M-1, \end{aligned} \tag{A.7}$$

that need to be iterated to find each of the roots z_r.

Since $g_G(z)$ has no poles for $|z| \le 1$, the numerator of the right-hand side of (23) should also have the zeros z_r, $r = 1, 2, \ldots, M-1$. Therefore, (23) is of the form

$$g_G(z) = \frac{K(z-1)\prod_{r=1}^{M-1}(z - z_r)}{C\sum_{k=0}^{N_{\max}} (\rho_V^k/k!) z^{B(k)} - z^M e^{\lambda_d(1-z)}}. \tag{A.8}$$

The constant K can be found by using the normalizing property $\lim_{z\to 1} g_G(z) = 1$, that is,

$$K \prod_{r=1}^{M-1} (1 - z_r) \lim_{z\to 1} \frac{z-1}{C\sum_{k=0}^{N_{\max}} (\rho_V^k/k!) z^{B(k)} - z^M e^{\lambda_d(1-z)}} = 1. \tag{A.9}$$

Therefore, the data backlog process probability generating function is as in (25).

B. DERIVATION OF EXPRESSION FOR MEAN NUMBER OF BACKLOGGED DATA PACKETS

In this appendix, we show that the mean number of backlogged data packets is as in (26).

Knowing the probability generating function of the data backlog process, its expected value can be obtained from the property $E[G_t] = \lim_{z\to 1} dg_G(z)/dz$, [9]. Consider first $\ln(g_G(z))$; from (25)

$$\begin{aligned} \ln\left(g_G(z)\right) &= \ln\left(\frac{M - \lambda_d - E[B_t]}{\prod_{r=1}^{M-1}(1 - z_r)}\right) + \ln(1-z) \\ &\quad + \sum_{r=1}^{M-1} \ln(z - z_r) - \ln\left(g_B(z) - z^M e^{\lambda_d(1-z)}\right). \end{aligned} \tag{B.10}$$

Then,

$$\begin{aligned} \frac{g_G'(z)}{g_G(z)} &= \sum_{r=1}^{M-1} \frac{1}{z - z_r} - \frac{1}{1-z} \\ &\quad - \frac{g_B'(z) - Mz^{M-1}e^{\lambda_d(1-z)} + \lambda_d z^M e^{\lambda_d(1-z)}}{g_B(z) - z^M e^{\lambda_d(1-z)}}. \end{aligned} \tag{B.11}$$

Taking $\lim_{z\to 1} dg_G(z)/dz$,

$$\begin{aligned} &\lim_{z\to 1} g_G'(z) \\ &= \sum_{r=1}^{M-1} \frac{1}{1 - z_r} \\ &\quad + \lim_{z\to 1} \left(- \frac{g_B'(z) - Mz^{M-1}e^{\lambda_d(1-z)} + \lambda_d z^M e^{\lambda_d(1-z)}}{g_B(z) - z^M e^{\lambda_d(1-z)}} - \frac{1}{1-z} \right). \end{aligned} \tag{B.12}$$

The second term on the right-hand side can be further reduced through algebraic operations and by considering

that $E[B_t] = \lim_{z\to 1} dg_B(z)/dz$ and $E[B_t^2] - E[B_t] = \lim_{z\to 1} d^2 g_B(z)/dz^2$ [9]:

$$\lim_{z\to 1}\left(-\frac{g_B'(z)-(M-\lambda_d z)z^{M-1}e^{\lambda_d(1-z)}}{g_B(z)-z^M e^{\lambda_d(1-z)}}-\frac{1}{1-z}\right)$$
$$=\frac{M-(M-\lambda_d)^2+g_V''(1)}{2(M-\lambda_d-g_B'(1))} \qquad \text{(B.13)}$$
$$=\frac{M-(M-\lambda_d)^2+E[B_t^2]-E[B_t]}{2(M-\lambda_d-E[B_t])}.$$

Then, we conclude that (26) holds.

REFERENCES

[1] J. E. Wieselthier and A. Ephremides, "Fixed- and movable-boundary channel-access schemes for integrated voice/data wireless networks," *IEEE Trans. Communications*, vol. 43, no. 1, pp. 64–74, 1995.

[2] J. E. Wieselthier and A. Ephremides, "Performance analysis of fixed- and movable-boundary channel-access schemes for integrated voice/data wireless networks," in *Proc. 12th Annual Joint Conference of the IEEE Computer and Communications Societies. Networking: Foundation for the Future (INFOCOM '93)*, vol. 3, pp. 1204–1213, San Francisco, Calif, USA, March–April 1993.

[3] D. J. Goodman, R. A. Valenzuela, K. T. Gayliard, and B. Ramamurthi, "Packet reservation multiple access for local wireless communications," *IEEE Trans. Communications*, vol. 37, no. 8, pp. 885–890, 1989.

[4] S. Nanda, D. J. Goodman, and U. Timor, "Performance of PRMA: a packet voice protocol for cellular systems," *IEEE Trans. Vehicular Technology*, vol. 40, no. 3, pp. 584–598, 1991.

[5] P. T. Brady, "A model for generating on-off speech patterns in two-way conversations," *Bell System Technical Journal*, vol. 48, no. 9, pp. 2445–2472, 1969.

[6] M. Alasti and N. Farvardin, "SEAMA: a source encoding assisted multiple access protocol for wireless communications," *IEEE Journal on Selected Areas in Communications*, vol. 18, no. 9, pp. 1682–1700, 2000.

[7] Qualcomm Inc., "Proposed EIA/TIA interim standard—wideband spread spectrum digital cellular system dual-mode mobile station-base station compatibility standard," Tech. Rep. 45.5, Telecommunications Industry Association (TIA), San Diego, Calif, USA, April 1992.

[8] A. Gersho and R. M. Gray, *Vector Quantization and Signal Compression*, Kluwer Academic Publishers, Boston, Mass, USA, 1992.

[9] A. Leon Garcia, *Probability and Random Processes for Electrical Engineering*, Addison Wesley, Reading, Mass, USA, 2nd edition, 1994.

[10] C. M. Barnhart, J. E. Wieselthier, and A. Ephremides, "An approach to voice admission control in multihop wireless networks," in *Proc. 12th Annual Joint Conference of the IEEE Computer and Communications Societies. Networking: Foundation for the Future (INFOCOM '93)*, vol. 1, pp. 246–255, San Francisco, Calif, USA, March–April 1993.

[11] H. Akimaru and K. Kawashima, *Teletraffic: Theory and Applications*, Springer-Verlag, Germany, 2nd edition, 1999.

[12] A. Ganz, Z. J. Haas, and C. M. Krishna, "Multi-tier wireless networks for PCS," in *Proc. IEEE 46th Vehicular Technology Conference. "Mobile Technology for the Human Race" (VTC '96)*, vol. 1, pp. 436–440, Atlanta, Ga, USA, April–May 1996.

Andres Kwasinski received his diploma in electrical engineering from the Buenos Aires Institute of Technology, Buenos Aires, Argentina, in 1992, and the M.S. and Ph.D. degrees from the University of Maryland, College Park, Md, in 2000 and 2004, respectively. Andres Kwasinski is currently a Research Associate in the Institute for Systems Research, University of Maryland, College Park, Md. During 1993, he worked for PECOM-NEC as telephone switches software developer and from 1994 to 1998 for Lucent Technologies in several capacities. His research interests are in the area of multimedia wireless communications, user-cooperative communications, cross-layer designs, wireless MAC protocols, and speech, audio, and video processing (especially in the area of signal compression).

Mehdi Alasti received the Ph.D. degree in electrical and computer engineering from the University of Maryland, College Park, Md, in 2001. He then worked at Zagros Networks, Inc. from 2001 till 2003, where he was a Principle Engineer architecting state-of-the-art switch fabrics and designing scheduling algorithms to support quality of service for high-speed switching systems. From July 2003 till January 2004, he was a Faculty Research Associate in the Department of Electrical and Computer Engineering, the University of Maryland, working on wireless communication networks. Since January 2004, he is with the Advanced Technology Group, Airvana Inc., as a Principle Engineer working on algorithms and protocols for high-speed wireless communication networks. He still conducts research in the area of communication networks and in particular the design algorithms and protocols for supporting quality of service in wireless networks. Mehdi Alasti is responsible for a number of inventions including his inventions in quality-of-service aware scheduling algorithms for crossbar switches, multiple access protocols for integrated voice-data wireless networks, and rate-based scheduling algorithms for wireless networks.

K. J. Ray Liu received the B.S. degree from the National Taiwan University in 1983, and the Ph.D. degree from UCLA in 1990, both in electrical engineering. He is a Professor in the Department of Electrical and Computer Engineering and Institute for Systems Research, University of Maryland, College Park. His research contributions encompass broad aspects of wireless communications and networking; information security; multimedia communications and signal processing; signal processing algorithms and architectures; and bioinformatics, in which he has published over 300 refereed papers. Dr. Liu is the recipient of numerous honors and awards including IEEE Signal Processing Society's 2004 Distinguished Lecturer, the 1994 National Science Foundation's Young Investigator Award, the IEEE Signal Processing Society's 1993 Senior Award (Best Paper Award), IEEE 50th Vehicular Technology Conference Best Paper Award, Amsterdam, 1999, and EURASIP 2004 Meritorious Service Award. He also received the George Corcoran Award in 1994 for outstanding contributions to electrical engineering education and the Outstanding Systems Engineering Faculty Award in 1996 in recognition of outstanding contributions in interdisciplinary research, both from the University of Maryland. Dr. Liu is a Fellow of IEEE. Dr. Liu is the Editor-in-Chief of IEEE Signal Processing Magazine and was the Founding Editor-in-Chief of EURASIP Journal on Applied Signal Processing.

Dr. Liu is a Board of Governor Member and has served as Chairman of Multimedia Signal Processing Technical Committee of IEEE Signal Processing Society.

Nariman Farvardin received the B.S., M.S., and Ph.D. degrees in electrical engineering from Rensselaer Polytechnic Institute, Troy, NY, in 1979, 1980, and 1983, respectively. Since January 1984, he has been with the Department of Electrical and Computer Engineering, the University of Maryland, College Park, Md, where he is currently a Professor and holds a joint appointment with the Institute for Systems Research. Dr. Farvardin is currently the Dean of the Clark School of Engineering, the University of Maryland. His research interests include information theory and coding, signal compression with applications to speech, image, and video coding and transmission, high-speed communication networks, and wireless systems and networks. Dr. Farvardin was the Associate Editor for Quantization, Speech/Image Coding of the IEEE Transactions on Communications from 1986 to 1990, and the Associate Editor for Source Coding of the IEEE Transactions on Information Theory from 1992 to 1995. In 1987, he received the Presidential Young Investigator Award from the National Science Foundation. Dr. Farvardin is a Fellow of the IEEE.

:: Open Access ::

EURASIP Journal on

Applied Signal Processing

http://www.hindawi.com/journals/asp/

Special Issue on

Digital Automatic Restoration of Audiovisual Archives

Call for Papers

Audiovisual archive material provides a unique record of key historic, artistic, and cultural elements of our civilization. The emergence of new multimedia and broadcasting outlets in the digital domain, including broadband internet as well as interactive and high-definition television services, has the potential of dramatically improving public access to cultural assets of unique educational and entertainment value. In addition to the above, renewed public interest in cultural heritage contributes to a favorable socioeconomic background for archive exploitation. Against this background, the level of public access today is limited by a number of prominent factors among which is the poor condition of material which is in urgent need of restoration. The complexity and associated cost of manual processes involved in a conventional restoration chain place considerable limitations on processing throughput rendering the restoration of entire collections an unrealistic proposition. Additionally, conventional restoration relies on the use of dedicated equipment which is of limited scope, partially use hazardous substances, expensive to purchase and maintain, and can only target a narrow range of artefacts. Ultimately the combined and inevitable effect of the above barriers is to deny the public all the benefits arising from unrestricted access as well as to prevent commercial exploitation plans to become a viable proposition. There is growing consensus that automatic restoration in the digital domain is a key enabling technology towards facilitating access to audiovisual archives for a number of reasons. By improving baseline picture quality and by reducing the perceptual impact of archive-related artefacts, restoration can meet viewers' aesthetic expectations and enrich the viewing experience. Moreover, the suppression of such artefacts has vital implications on the efficiency of video coding algorithms used in the television and multimedia distribution chains such as MPEG-2/4 and H.264. Finally, since restoration processes almost invariably result in the enhancement of semantic content, they are also likely to contribute to more efficient content-driven management of pictorial databases and archives.

The proposed special issue on *Digital Automatic Restoration of Audiovisual Archives* is intended to provide a focal point for applied digital signal processing research in the field of audiovisual restoration.

Topics of interest include but are not limited to the following:

- Signal processing algorithms for the restoration of global visual archive impairments
- Signal processing algorithms for the restoration of local visual archive impairments
- Spatial-domain and motion-compensated approaches in visual restoration
- Signal processing algorithms for the restoration of audio impairments
- Statistical approaches in visual and audio restoration
- Exemplar-based impairment concealment and synthesis
- Restoration algorithms in forward and inverse standards conversion
- Impact of restoration on digital video compression performance
- Signal processing algorithms for the restoration of still images and digitized photographic material

Authors should follow the EURASIP Journal on Advances in Signal Processing manuscript format described at http://www.hindawi.com/journals/asp/. Prospective authors should submit an electronic copy of their complete manuscript through the journal Manuscript Tracking System at http://mts.hindawi.com/, according to the following timetable:

Manuscript Due	October 1, 2007
First Round of Reviews	December 1, 2007
Publication Date	March 1, 2008

Guest Editors

Theodore Vlachos, Centre for Vision, Speech and Signal Processing, School of Electronics and Physical Sciences, University of Surrey, Guildford GU2 7XH, UK; t.vlachos@surrey.ac.uk

Anil Kokaram, Sigmedia Group, Department of Electronic & Electrical Engineering, Printing House, Trinity College, Dublin 2, Ireland; akokaram@tcd.ie

Bernard Besserer, Laboratoire L3i, Pôle Sciences et Technologie, Université de La Rochelle, 17042 La Rochelle Cedex 1, France; bernard.besserer@univ-lr.fr

Peter Schallauer, Institute of Information Systems & Information Management, JOANNEUM RESEARCH Forschungsgesellschaft mbH, 8010 Graz, Austria; peter.schallauer@joanneum.at

Hindawi Publishing Corporation
410 Park Avenue, 15th Floor, #287 pmb, New York, NY 10022, USA

HINDAWI

EURASIP Book Series on Signal Processing and Communications

Advances in Nonlinear Signal and Image Processing

Edited by: Stephen Marshall and Giovanni L. Sicuranza

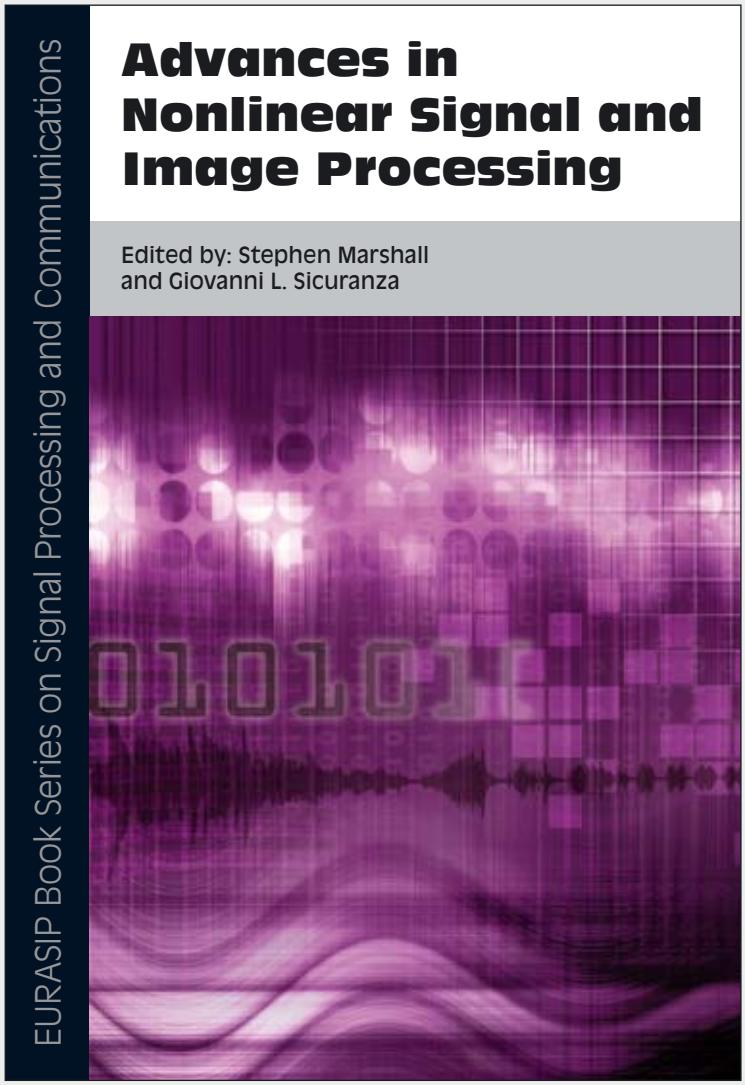

The interest in nonlinear methods in signal processing is steadily increasing, since nowadays the advances in computational capacities make it possible to implement sophisticated nonlinear processing techniques which in turn allow remarkable improvements with respect to standard and well-consolidated linear processing approaches.

The aim of the book is to present a review of emerging new areas of interest involving nonlinear signal and image processing theories, techniques, and tools.

More than 30 leading researchers have contributed to this book covering the major topics relevant to nonlinear signal processing. These topics include recent theoretical contributions in different areas of digital filtering and a number of applications in genomics, speech analysis and synthesis, communication system, active noise control, digital watermarking, feature extraction, texture analysis, and color image processing.

The book is intended as a reference for recent advances and new applications of theories, techniques, and tools in the area of nonlinear signal processing. The target audience are graduate students and practitioners working on modern signal processing applications.

EURASIP Book Series on SP&C, Volume 6, ISBN 977-5945-37-2 .
Please visit http://www.hindawi.com/spc.6.html for more information about the book. To place an order while taking advantage of our current promotional offer, please contact books.orders@hindawi.com